Chalcogenide Letters Vol. 8, No. 3, March 2011, p. 187 – 198

PROSPECTS OF BACK CONTACTS WITH BACK SURFACE FIELDS IN HIGH EFFICIENCY $Zn_xCd_{1-x}S$ /CdTe SOLAR CELLS FROM NUMERICAL MODELING

MD. SHARAFAT HOSSAIN[a], NOWSHAD AMIN[a,b], TAKHIR RAZYKOV[b]
[a]*Department of Electrical, Electronics and System Engineering,*
Faculty of Engineering and Built Environment,
Universiti Kebangsaan Malaysia (UKM), 43600 Bangi, Selangor, Malaysia
[b]*Solar Energy Research Institute*
Universiti Kebangsaan Malaysia (UKM), 43600 Bangi, Selangor, Malaysia

Zinc Cadmium Sulfide ($Zn_xCd_{1-x}S$) thin films have been recognized as good candidates in photovoltaic devices acting as wide-bandgap window layer. Results of numerical analysis using AMPS-1D simulator in exploring the possibility of ultra thin, high efficiency and stable $Zn_xCd_{1-x}S$ /CdTe solar cells are presented. A baseline structure of CdS/CdTe cell was explored in this work with reduced CdTe absorber layer and $Zn_xCd_{1-x}S$ has been replaced to CdS as window layer, where 1 µm thin CdTe and 80 nm $Zn_xCd_{1-x}S$ layers showed reasonable efficiencies over 18%. The viability of 1 μm CdTe absorber layer together with possible back surface field (BSF) in $Zn_xCd_{1-x}S$/CdTe cells was investigated. Moreover, the variation of x in $Zn_xCd_{1-x}S$ was analysed for high efficient cell and the optimal value of x was found to be 8%. The proposed structure of $SnO_2/Zn_2SnO_4/CdS/CdTe/As_2Te_3/Cu$ showed the highest conversion efficiency of 18.9% (*Voc* = 0.92 V, *Jsc* = 24.98 mA/cm^2 and *FF* = 0.82). However, other proposed structures such as $SnO_2/Zn_2SnO_4/CdS/CdTe/Sb_2Te_3/Mo$ and SnO_2/Zn_2SnO_4/CdS/CdTe/ZnTe/Al showed better stability at higher operating temperatures. Moreover, it was found that the cells normalized efficiency linearly decreased with the increased temperature at lower gradient, which eventually indicates better stability of the proposed ultra thin $Zn_xCd_{1-x}S$ /CdTe cells.

(Received March 11, 2011; Accepted March 25, 2011)

Keywords: $Zn_xCd_{1-x}S$ /CdTe solar cell, Ultra thin CdTe absorber, AMPS 1D, Normalized efficiency, Stability

1. Introduction

Polycrystalline CdTe shows greater promises for the development of cost effective, efficient and reliable thin film solar cells. CdTe based PV modules are currently entering mass production, but still there are potential scopes remained for improvement of the cell performance, materials usage and cell stability. The main technical issues of CdTe cells are related to the lesser material usage, stable back contact and appropriate window layer. The polycrystalline CdTe has a high absorption coefficient of over 5×10^5/cm, which means that all the potential photons with energy greater than the bandgap (E_g) can be absorbed within a very thin CdTe absorber layer. Moreover, CdTe has a direct optical bandgap of 1.45 eV which is very close to the optimum bandgap for solar cells. Hence, the lesser thickness required for an absorbing layer can lead to reduced cell material usage and lower cost of fabrication.

---

*Corresponding author: sharafat57@gmail.com

The CdTe thin film solar cells have shown long-term stable performance [1-2] and high efficiency under AM1.5 illumination for global usage. In traditional CdTe solar cells CdS is popularly used as a window material and as an n-type heterojunction partner to p-CdTe. Since the bandgaps of CdTe and CdS are 1.5 and 2.4 eV, respectively, it means that only photons with energies within this range reach CdTe layer where they contribute to the cell's photocurrent. The coefficients of absorption in II-VI compounds in the spectrum window are high [3], which is about 10^4 to 10^5 cm^{-1}. As a result, the electron hole pair (EHP) generated by higher energy photons in the n-CdS layer takes place at the surface far away from the depletion region where the generated EHP can be collected. Thus, the EHPs are often lost to surface recombination current. Consequently, the dark current is increased which reduces the useful current delivered by the cell to a load. To decrease the absorption and minimize the surface recombination current in CdS/CdTe cells, reducing the thickness of CdS layer [4] to less than 1000 Å is routinely done. At this thickness they appear to be low yield due to increase in the shunting probability. Below 700 Å, there is a general degradation [4] in the cell performance owing to considerable decrease in shunt resistance and due to excessive pinhole formation across the heterojunction which can adversely affect the device open-circuit voltage (*Voc*) and fill factor (*FF*). It should have, therefore, been more appropriate to use a thick layer like ZnS film with 3.7 eV bandgap as a window, but there are several negative aspects related with this scheme. First, ZnS is exceedingly resistive and very hard to dope [5] and could considerably increase the cell's series resistance. Second, the lattice mismatch between ZnS and CdTe is about 16%, making it an inferior heterojunction partner to CdTe compare to CdS.

Considering the above discussion, we have chosen $Zn_xCd_{1-x}S$ as an alternative window structure in CdTe solar cells. It has been used as a potential window layer to form heterojunction solar cells with Si [6], Cu_xS [7], $CuInSe_2$ [8], $CuGaSe_2$ [9], $Cu(In,Ga)Se_2$ (CIGS) [10] and CdTe [11] for its large and variable bandgap between 2.42 and 3.54 eV. The lattice constant of $Zn_xCd_{1-x}S$ lies between CdS and ZnS [12] and the electron affinity can be made closer to CdTe by controlling the concentration of Zn [13]. However, in CdS/CdTe interface the electron affinity, lattice constant and thermal mismatches result in the formation of high density of interface states which reduce the *Voc* and accordingly the conversion efficiency of the cell [14]. The conduction and valence band edges of this material lie between [12] those of ZnS and CdS depending on the Zn or Cd content. The addition of Zn to CdS improves the *Voc* and Short circuits current (*Jsc*) in heterojunction devices as a result of the decrease of absorption losses in the window layer [15, 16]. Under AM1.5 illumination, $Zn_xCd_{1-x}S$ is transparent to this spectrum [17], the EHPs generated by the higher energies photons now well removed from the cell surface, are no longer lost to surface recombination. Instead, they are separated and collected by the assistance of the field present in this region. It enhances the spectral response [18, 19, 20] in the short wavelength region without compromising the layer thickness. The outcome therefore is a strong spectral response of the solar cell in almost all AM1.5 spectrums resulting in higher efficiency $Zn_xCd_{1-x}S$/CdTe solar cell.

Various methods have been used to produce $Zn_xCd_{1-x}S$ films, including photochemical deposition [21], co-evaporation [22], chemical spray deposition [23] , chemical bath deposition [24], closed-space sublimation (CSS) [25]. Most of the published papers about $Zn_xCd_{1-x}S$ focused on its physical and chemical properties. There are only limited reports that described the application of $Zn_xCd_{1-x}S$ in CdTe solar cells. Zhou et al [24] found a maximum efficiency of 15.7% (*Voc* = 0.84 V, *Jsc* = 24.80 mA/cm^2, *FF* = 0.76), Fahrenbruch et al [26] obtained a maximum efficiency of 6.3 % for $Zn_xCd_{1-x}S$/CdTe cells. Suyama et al [27] reported on screen printed ZnCdS/CdTe solar cells and obtained a maximum open-circuit voltage of 0.74 V. Inspite of the promising theoretical conversion efficiencies, attempts to fabricate and characterize $Zn_xCd_{1-x}S$ /CdTe cells are very limited. Hence, there are scopes to increase the efficiency of $Zn_xCd_{1-x}S$ /CdTe cells by improving *Voc, Jsc* and *FF* with suitable front contact buffer layer (ZnO/Zn_2SnO_4) and back contact buffer layer which are termed as BSF (As_2Te_3, Sb_2Te_3, ZnTe) utilizing AMPS 1D (Analysis of Microelectronic and Photonic Structures) [28] simulator and the obtained results are discussed in the following sections.

2. Modeling and simulation

Numerical modeling is increasingly being used to obtain insight into the details of the physical operation of solar cells. Modeling and simulation were done using AMPS-1D simulator to explore the possibilities of thinner CdTe absorber and $Zn_xCd_{1-x}S$ window layers with high conversion efficiency. The AMPS-1D program has been developed to realistically simulate the electrical characteristics of the thin film heterojunction solar cells. It has been tested for thin film CdTe and CIGS solar cells [29]. The baseline case of CdTe cell [30] was utilized to approximate the highest efficiency CdS/CdTe solar cells at that time, and it was modified in this work to explore the possibility of efficient ultra thin $Zn_xCd_{1-x}S$/CdTe cells with suitable BSF. Many researchers have carried out simulations with CdTe based solar cells, and a list can be found in the references given in the review paper by M. Burgelman et al. [31]. Fig. 1 illustrates the CdTe baseline case structure and modified (Glass/SnO_2/ZnO/ $Zn_xCd_{1-x}S$/CdTe/BSF/Metal) structure for higher conversion efficiency.

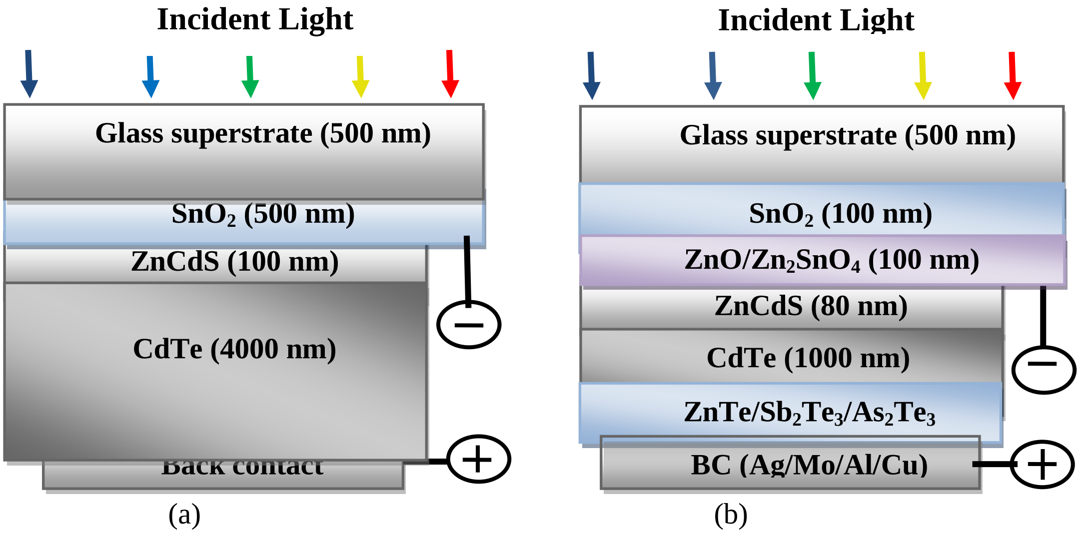

Fig. 1: Structures of the CdTe solar cells: (a) Conventional baseline case structure and (b) Modified structure for higher performance.

It is clear from Fig. 1 that the modified structure has an extra layer (ZnO or Zn_2SnO_4) in between SnO_2 and $Zn_xCd_{1-x}S$ layer to achieve higher performances. Thus, the front contact consists of SnO_2 plus a buffer layer of ZnO or Zn_2SnO_4. The doping concentration (up to 10^{14} cm^{-3}) used in the baseline case was changed to (up to 10^{15} cm^{-3}) for today's achievable values for CdTe material. Proper BSF were inserted to overcome rollover effect, instability at higher operating temperature and to reduce minority carrier recombination loss at the back contact in the proposed ultra thin $Zn_xCd_{1-x}S$/CdTe cells. Cheaper metals (Ag/Al/Mo) were used as final back contact material in the proposed cells for the low cost aspect. The number of parameters that can be varied in a particular solar cell model is larger than 50 [31]. Obviously, a problem with 50 variables is too ambiguous and tedious to solve reliably. It is therefore necessary to minimize the number of variable parameters by fixing many of them at reasonable values. It was a tough challenge to choose the appropriate parameters to be used for the different layers of the cells. Many of them depend on fabrication techniques and deposition methods and can thus vary even between devices fabricated in the same batch. Table 1 shows the significant material parameters used in this modeling, which were selected based on literature values, theory, or in some case, reasonable estimations.

Table 1: Material parameters used in simulation.

Parameter	n-SnO_2	n-ZnO/n-Zn_2SnO_4	p-CdTe	ZnTe/Sb_2Te_3/As_2Te_3	Comments and references
W (μm)	0.01- 0.5	0.02- 0.5	0.1- 6.0	0.01- 0.5	Theory & estimations
$\varepsilon/\varepsilon_o$	9.0	9.0	9.4	14/55/20	[30, 32, 33, 34]
μ_c (cm^2/Vs)	100	100/32	320	70/1094/500	[30, 34, 35, 36]
μ_p (cm^2/Vs)	25	25/03	40	50/320/210	[30, 34, 35, 36]
n, p (cm^{-3})	10^{17}	10^{19}	5×10^{15}	7.5×10^{19}	[30, 37, 38]
E_g (eV)	3.6	3.0/3.35	1.45	2.25/0.3/0.6	[30, 37, 38]
N_C (cm^{-3})	2.2×10^{18}	2.0×10^{18}	8.0×10^{17}	7.5×10^{17}	[30, 37, 38]
N_V (cm^{-3})	1.8×10^{19}	1.5×10^{19}	1.8×10^{19}	1.5×10^{19}	[30, 37, 38]
χ (eV)	4.50	4.35/4.50	4.28	3.65/4.15/4.0	[30, 35, 36, 37, 38]

In this modeling, all the layer thickness were varied: the CdTe layer from 100 nm up to 6 μm, $Zn_xCd_{1-x}S$ window layer from 25 nm to 200 nm, ZnO or Zn_2SnO_4 buffer layer from 20 nm to 500 nm and BSF layer from 10 nm to 500 nm while keeping all other cell parameters at fixed value as shown in Table 1.

3. Results and discussion

3.1 Optimization of the value of x in $Zn_xCd_{1-x}S$ Window Layer

The baseline case for optimizing the composition of x was the structure of CdTe cell [30] in which CdS is replaced by $Zn_xCd_{1-x}S$ and doping concentration (10^{14} cm^{-3}) has been changed to (10^{15} cm^{-3}). Numerical simulation has been done to see the effect of Zn content on conversion efficiency from x=0 to x=1 using the parameters from Table 2 which was adopted from [19, 39, 40, 41, 42, 43].

Table 2 Material properties of n-$Zn_xCd_{1-x}S$ for simulation.

Parameter	X=0.05	X=0.08	X=0.1	X=0.2	X=0.3	X=0.5	X=0.6	X=0.8
W (μm)	0.1	0.02-0.3	0.1	0.1	0.1	0.1	0.1	0.1
$\varepsilon/\varepsilon_o$	9.3	9.3	9.3	9.3	9.3	9.3	9.3	9.3
μ_c (cm^2/Vs)	100	100	95	85	75	70	65	60
μ_p (cm^2/Vs)	40	40	35	30	25	20	15	10
n, p(cm^{-3})	3.0×10^{16}	2.5×10^{16}	2.5×10^{16}	1.7×10^{16}	1.6×10^{16}	4.1×10^{15}	2.5×10^{15}	1.7×10^{15}
E_g (eV)	2.48	2.50	2.55	2.58	2.64	2.70	3.07	3.33
N_C (cm^{-3})	2.1×10^{18}	2.1×10^{18}	2.1×10^{18}	2.1×10^{18}	2.1×10^{18}	2.1×10^{18}	2.1×10^{18}	2.1×10^{18}
N_V (cm^{-3})	1.7×10^{19}	1.7×10^{19}	1.7×10^{19}	1.7×10^{19}	1.7×10^{19}	1.7×10^{19}	1.7×10^{19}	1.7×10^{19}
χ (eV)	4.47	4.46	4.44	4.38	4.32	4.26	4.14	4.02

it was noticed that for low content of Zn (≤ 10%), the conversion efficiency (Eff), *Voc*, and *FF* are higher than for high content of Zn (> 10%) and Jsc was increased for x=0 to x=0.1 and almost same up to x=0.35 then started to decrease up to x=1. A conversion efficiency of 17.9% (*Voc* = 0.91 V, *Jsc* = 24.7 mA/cm^2 and *FF* = 0.8) for x=0.05 and 17.7% (*Voc* = 0.92 V, *Jsc* = 24.4 mA/cm^2 and *FF* = 0.8) for x=0.08. The electrical resistivity of $Zn_xCd_{1-x}S$ layer increases from 1 Ω-cm (x=0) to 10^{10} Ω-cm (x=1) [30, 39]. In consideration to fabrication complexity and simulation results, we have selected x=0.08 for this work. In the following section, $Zn_xCd_{1-x}S$ has been replaced to $Zn_{0.08}Cd_{0.92}S$ for our proposed cell.

3.2 CdTe Absorber Layer and $Zn_{0.08}Cd_{0.92}S$ Window Layer Optimization

The conventional CdTe baseline structure [30] (SnO_2/CdS/CdTe) was the starting point of this analysis in where CdS was replaced by $Zn_{0.08}Cd_{0.92}S$. The conversion efficiency of 15.0% (*Voc* = 0.86 V, *Jsc* = 24.47 mA/cm^2, *FF* = 0.71) was found from the baseline case structure where CdTe was 4 µm, $Zn_{0.08}Cd_{0.92}S$ was 100 nm and Ag as the final back contact metal. When the today's achievable CdTe doping concentration (5×10^{16}) and life time (1.6 ns) were adopted the cell conversion efficiency increased to 17.4% (*Voc* = 0.9 V, *Jsc* = 24.5 mA/cm^2, *FF* = 0.8). This improvement was achieved mainly from increased *Voc* and *FF* due to higher CdTe absorber doping concentration and life time than the baseline case cell. It is noteworthy that in most high efficiency CdTe solar cells, the CdTe absorber layer is purposely set at 5 µm and above to avoid pinhole formation and uniformity limitation.

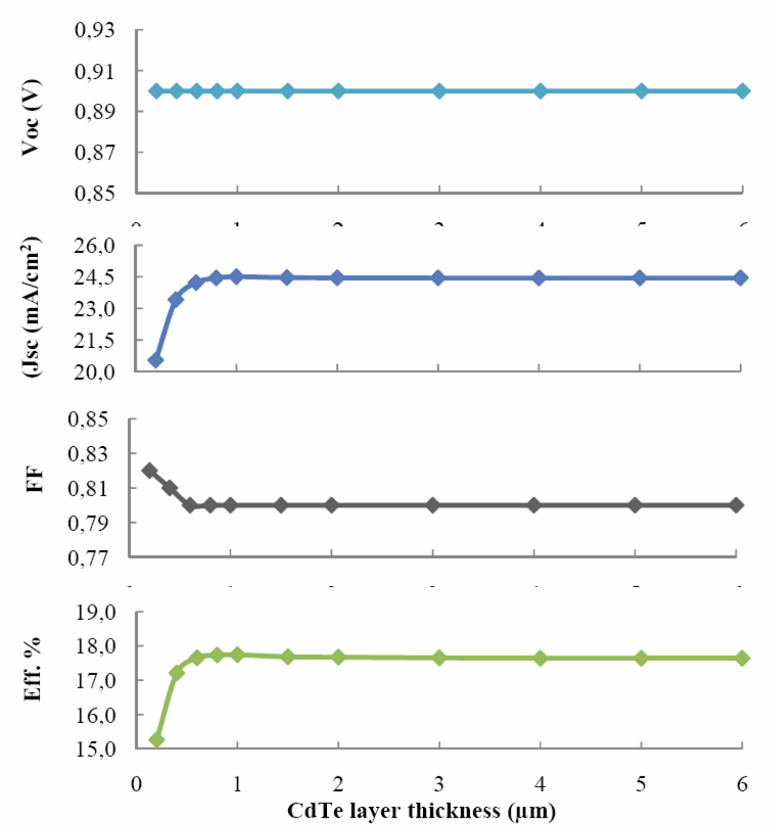

Fig. 2: Effect of CdTe film thicknesses on cell parameters.

Theoretically the minimum thickness required is approximately 2 µm for CdTe layer to absorb 99% of the incident photons with energy greater than E_g [44]. However, further numerical analysis was done to reduce the thickness of CdTe and $Zn_{0.08}Cd_{0.92}S$ layers aiming to conserve the materials usages and cost of cell production. The CdTe absorber thickness was varied from 100 nm to 6000 nm to explore thinner CdTe absorber layer using AMPS-1D simulator the simulated results are shown in Fig. 2.

It is clear from the Fig. 2 that all the solar cell output parameters were unaffected around the CdTe thickness of 1 µm. Further reduction of CdTe thickness from 1 µm it has shown that *Jsc* decreased slowly but the *Voc* remained almost unaffected and *FF* increased bellows 600 nm. At the lower value of CdTe thickness (<0.5 µm) the *Jsc* decreased sharply due to the minority carrier diffusion length is critically shorter but *FF* showed a little increased value due to the reduction of bulk resistance for CdTe material. As a combined effect, efficiency decreased with reduced CdTe thickness below 1 µm, which indicated that selection of 1 µm CdTe absorber is safe. It can be seen from the electric field distribution of Fig. 3 for the 1 µm thick CdTe cell that the electric field diminishes before 1 µm of CdTe thickness. The charge depletion extends nearly 0.6 µm into the CdTe layer. If the thickness of the CdTe layer is restricted to smaller values (< 0.6 µm), then the layer is said to be 'fully depleted'. While collection in a fully depleted device is usually good due to the field strength at all positions but built-in potential and hence device voltage, tend to be reduced. The 1 µm thick CdTe cell shows acceptable conversion efficiency of 17.4% (*Voc* = 0.90 V, *Jsc* = 24.5 mA/cm^2, *FF* = 0.8).

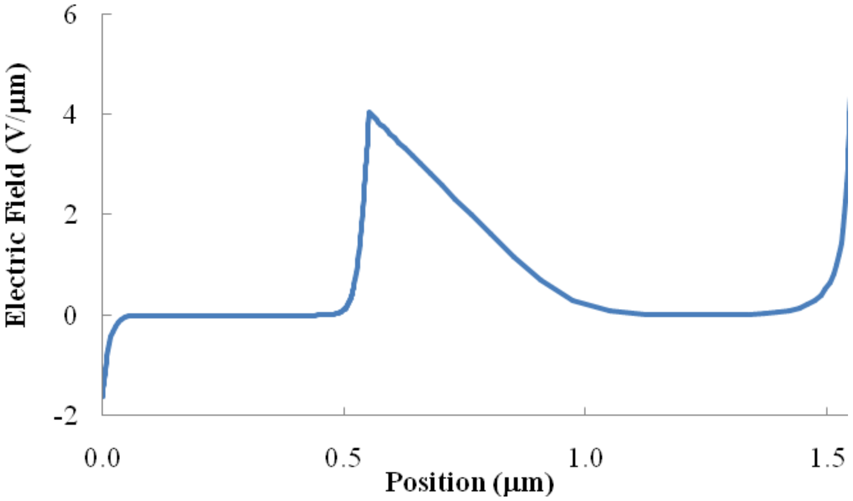

Fig. 3: Effect of CdTe thicknesses on electric field distribution.

However, there are possibility of increasing the overall cell conversion performance if the $Zn_{0.08}Cd_{0.92}S$ window layer thickness (100 nm) can be reduced further with insertion of a suitable buffer layer in between SnO_2 and $Zn_{0.08}Cd_{0.92}S$ layer. Moreover, the buffer layer might constitute a barrier against diffusion of unwanted species from the substrate and SnO_2 layer to $Zn_{0.08}Cd_{0.92}S$. It was found that when $Zn_{0.08}Cd_{0.92}S$ film thickness has been reduced to explore thinner $Zn_{0.08}Cd_{0.92}S$ layer that improves mainly *Jsc* and consequently cell conversion efficiency but *Voc* and *FF* are not so much affected. The spectral response (SR) of $Zn_{0.08}Cd_{0.92}S$ layer thickness variation from 25 nm to 200 nm is shown in Fig. 4 from where the improvement of *Jsc* will be clearer.

It is evident that when the operating wavelength is below 510 nm the quantum efficiency (QE) was significantly affected with the increasing $Zn_{0.08}Cd_{0.92}S$ layer thickness. This affected mainly *Jsc* and finally the conversion efficiency of the cell. This result is in good agreements with other published works [35]. However, considering the fabrication constraint, the $Zn_{0.08}Cd_{0.92}S$ film thickness of 80 nm was selected with conversion efficiency of 17.8% (*Voc* = 0.9 V, *Jsc* = 24.7 mA/cm^2, *FF* = 0.8). Thus, it is very clear that the improved cell performance has been achieved mainly due to the improvement of *Jsc*.

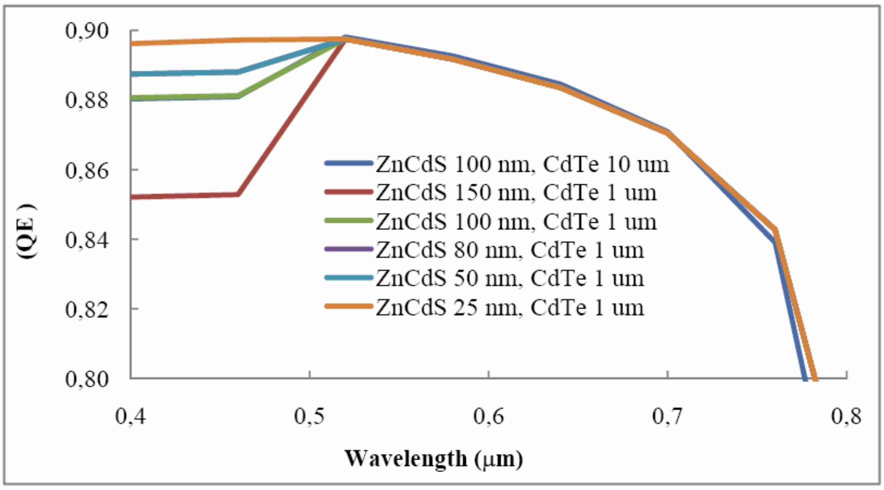

Fig. 4: Effect of $Zn_{0.08}Cd_{0.92}S$ thicknesses on the cell spectral response.

3.2 Insertion of ZnO/Zn_2SnO_4 Buffer Layer

The $Zn_{0.08}Cd_{0.92}S$ layer was reduced to 80 nm, for such a thin $Zn_{0.08}Cd_{0.92}S$ window layer it was necessary to insert front contact buffer layer for further improvement of the cell performance. A high resistive buffer layer of suitable material (ZnO or Zn_2SnO_4) was inserted in between SnO_2 and $Zn_{0.08}Cd_{0.92}S$ window layer. Now the front contact of the proposed cells consist of a highly conducting layer of SnO_2 material as TCO for low resistance due to contact and lateral current collection and a much thinner high resistivity layer of a suitable buffer material (ZnO or Zn_2SnO_4). Further numerical analysis was done using AMPS-1D to investigate the cells performances with proposed buffer layers (ZnO or Zn_2SnO_4). The buffer layer were inserted in the designed CdTe cell with 1 µm CdTe, 80 nm $Zn_{0.08}Cd_{0.92}S$, 100 nm SnO_2 layers and all other parameter as in Table 1& 2. Moreover, I-V characteristics obtained from AMPS-1D simulation with buffer layers are shown in Fig. 5.

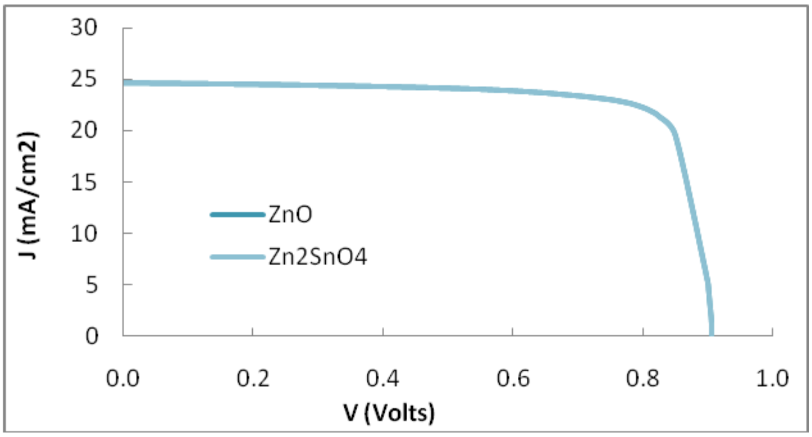

Fig. 5: Effect of ZnO and Zn_2SnO_4 on cell I-V characteristics.

ZnO insertion has shown almost the same result with Zn_2SnO_4 insertion as the material properties are very close to each other. With the insertion of ZnO and Zn_2SnO_4 the I-V curve had shown higher shunt and series resistances. Higher shunt resistance is desired for the better performance of cells but higher series resistance is undesirable which might be reduced the *FF*. The cell output characteristics are independent of the ZnO/Zn_2SnO_4 thickness from 20 nm up to 500 nm. Moreover, it was observed that the SR of the cells were unaffected by the ZnO/Zn_2SnO_4

thickness variation from 20 nm to 500 nm, meaning that a very thin buffer layer is adequate for the purpose. Considering the reality in fabrication, the ZnO/Zn_2SnO_4 buffer layer thickness was selected 100 nm with maximum cell conversion efficiency of 18.1%. It is noticeable here that with the insertion of buffer layer the efficiency of the cells did not improves a bit and the SnO_2 layer was reduced to 100 nm from 500 nm, which means that reduced material use can reduce the production cost. However, until now the proposed cells are with Ag as the final back contact material. There are scopes for further improvement of cell's performance with BSF layer and with other suitable back contact metals.

3.3 Insertion of BSF and Cells Stability

One of the major differences of thin cells compared to the thicker ones is that the absorber/back contact interface is now located closer to the p-CdTe and n-$Zn_{0.08}Cd_{0.92}S$ junction, and the choice of the back contact material therefore has a high impact on the cell performance. A stable back contact that is not significantly rectifying is essential for good performance and long term stability of $Zn_{0.08}Cd_{0.92}S$/CdTe cells. The formation of a low resistance, low barrier back contact is one of the most challenging aspects for high performance CdTe based solar cells.

Further numerical analysis has been done with the proposed ultra thin cell ($SnO_2/Zn_2SnO_4/$ $Zn_{0.08}Cd_{0.92}S$/CdTe/Ag) aiming to explore the performances with three different BSF materials. The cells with 1 μm CdTe, 80 nm $Zn_{0.08}Cd_{0.92}S$, 100 nm SnO_2 and 100 nm BSF layers were simulated using AMPS-1D; the obtained results are summarized in Table 3.

Table 3: Output parameters of different cells with BSF.

Different Cell Structures	Voc (V)	Jsc (mA/cm²)	FF	Eff. (%)
Glass/$SnO_2/Zn_2SnO_4/$ $Zn_{0.08}Cd_{0.92}S$/CdTe/Ag	0.90	24.61	0.81	18.1
Glass/$SnO_2/Zn_2SnO_4/$ $Zn_{0.08}Cd_{0.92}S$/CdTe/ZnTe/Al	0.90	24.93	0.71	16.0
Glass/$SnO_2/Zn_2SnO_4/$ $Zn_{0.08}Cd_{0.92}S$/CdTe/Sb_2Te_3/Mo	0.91	24.95	0.76	17.5
Glass/$SnO_2/Zn_2SnO_4/$ $Zn_{0.08}Cd_{0.92}S$/CdTe/As_2Te_3/Cu	0.92	24.98	0.82	18.9

It is evident from Table 3 that the proposed best cell without any BSF layer shows conversion efficiency of 18.1%, which is a high value for $Zn_{0.08}Cd_{0.92}S$/CdTe cells. When ZnTe is inserted as a BSF the conversion efficiency drops as the *FF* was strongly affected but the *Jsc* improved a bit due to reduced minority carrier recombination loss at the back contact. The reduction in *FF* might be attributed to the barrier developed for holes in the valance band and *Jsc* improved due to electrons reflected back from the conduction band, which will be clearer from the band diagram of the cells (Fig. 6). When Sb_2Te_3 was inserted as BSF layer the *FF* and conversion efficiency improved better than that of ZnTe BSF because there is no barrier for holes at the valance band. The As_2Te_3 BSF produced best cell performances and highest conversion efficiency of 18.9%. The improvement in efficiency of this cell came from the improvement of all the cell output parameters like *FF*, *Voc* and *Jsc.*

Fig. 6 shows the band diagram of the proposed cells without BSF, with ZnTe/Al BSF, Sb_2Te_3/Mo BSF and As_2Te_3/Al BSF at zero voltage biasing. The front contacts of the cells are same ($SnO_2/Zn_2SnO_4/$ $Zn_{0.08}Cd_{0.92}S$) with a band discontinuity of 0.22 eV at $Zn_{0.08}Cd_{0.92}S$-CdTe junction. Without any BSF layer it was found that there is a rectifying back contact with p-CdTe and Ag material which might be responsible for 'rollover' of this cell. Smoother collections of holes are anticipated as there is no barrier in the conduction band for all the proposed cells except the cell with ZnTe BSF.

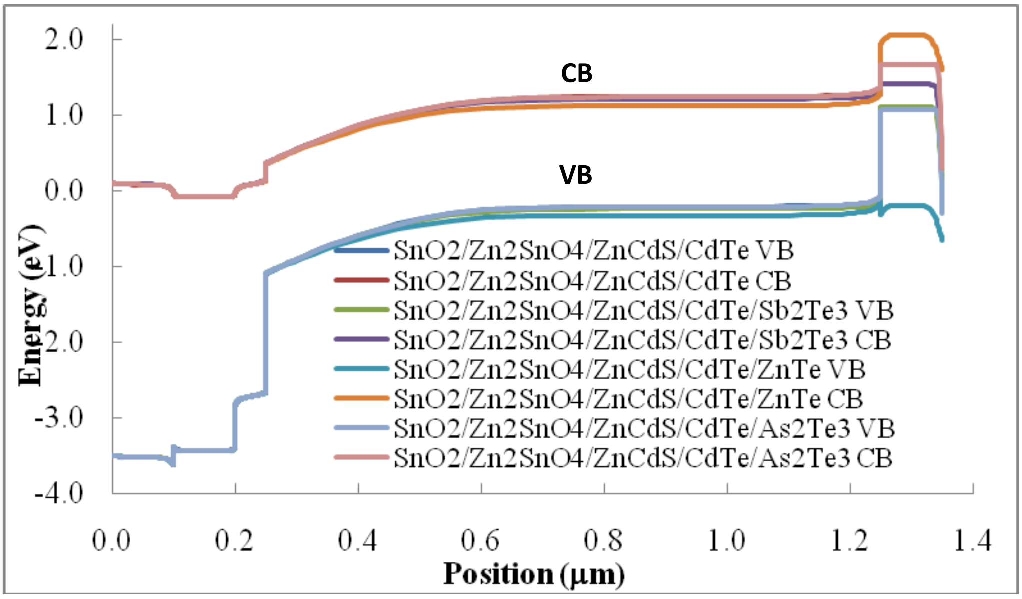

Fig. 6. Band diagram of the proposed cells.

It is clear from the figure that the ZnTe has shown a barrier at the valance band of CdTe and ZnTe interface which might be responsible for its lower FF and conversion efficiency. All the BSF will effectively reflect back the electrons from the conduction band interface of CdTe-BSF towards the front contact as there is adequate barrier height in the conduction band of all the cells with BSF. For Sb_2Te_3 the barrier height is 0.2 eV, for As_2Te_3 the barrier height is 0.45 eV and for ZnTe barrier height is 0.8 eV. Due to these barrier heights, cells with BSF have shown higher *Jsc*. It seems that 0.2 eV BSF is enough for the purpose of reflecting back the electrons towards front contact. Moreover, J-V characteristics of all the proposed cells are shown in Fig. 7.

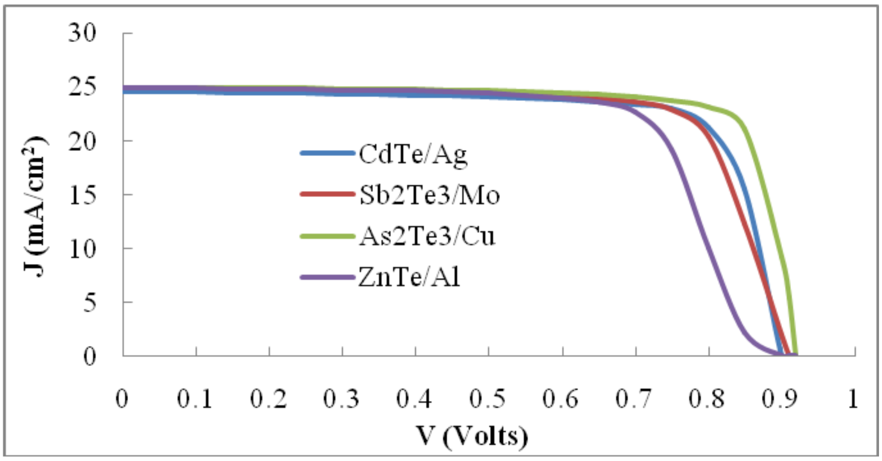

Fig. 7. J-V characteristics of the proposed cells.

As can be seen in Fig. 7, the structure with BSF shows higher *Jsc* than the cell without BSF, while the cell with ZnTe/Al shows higher *Jsc* but poor FF due to the barrier for holes in the valance band and higher series resistance added by the bulk resistance of the higher bandgap and lower dielectric property of the ZnTe material. The Sb_2Te_3/Mo shows moderate cell output parameters. In this analysis As_2Te_3/Cu has shown improved performances better than Sb_2Te_3/Mo and ZnTe/Al. Before any final conclusion on the BSF results, there is need to investigate the stability of the cells at higher operating temperatures. An investigation was conducted utilizing AMPS-1D at operating temperature ranged from 25°C to 100°C for the proposed cells. The results are shown in Fig. 8 and it can be seen that the cells with ZnTe have shown better overall stability than other proposed cells.

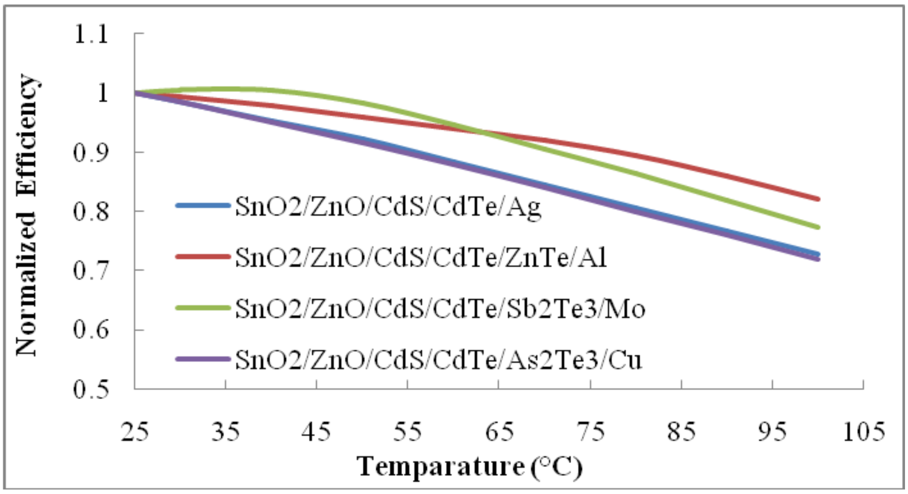

Fig. 8. Effect of operating temperature on the cells performances.

4. Conclusion

A highly efficient 18.9% (*Voc* = 0.92 V, *Jsc* = 24.98 mA/cm^2 and *FF* = 0.82) ultra thin $Zn_{0.08}Cd_{0.92}S$/CdTe solar cell with 1 µm of CdTe, 80 nm of $Zn_{0.08}Cd_{0.92}S$, 100 nm SnO_2, 100 nm of Zn_2SnO_4 and 100 nm of As_2Te_3 has been obtained. It was found that the reduced $Zn_{0.08}Cd_{0.92}S$ layer thickness improves the spectral response of the cell at the blue region with suitable buffer layer of ZnO/Zn_2SnO_4. The Zn_2SnO_4 buffer layer insertion showed almost the same results with ZnO insertion. It has also been found that SnO_2/Zn_2SnO_4 front contact with Sb_2Te_3/Mo and As_2Te_3/Cu as BSF are suitable contacts for higher efficiency (>17.5%) and stable ultra thin $Zn_{0.08}Cd_{0.92}S$/CdTe cells. Moreover, the simulation result of cell operating temperature has shown the stability. The structure of (SnO_2/Zn_2SnO_4/ $Zn_{0.08}Cd_{0.92}S$/CdTe/ZnTe/Al) achieved the best stability with a linear thermal coefficient of -0.3%/°C. From the consideration of both efficiency and stability, structures with As_2Te_3/Cu (SnO_2/Zn_2SnO_4/ $Zn_{0.08}Cd_{0.92}S$/CdTe/As_2Te_3/Cu) proved to be comparable to other reported cells, and the proposed cells can be investigated using standard fabrication techniques.

Acknowledgments

This work has been supported through research Grant by the department of Electrical, Electronic & System Engineering and Solar Energy Research Institute (SERI), UKM, Malaysia.

References

[1] D. L. Batzner, A. Romeo, H. Zogg, R. Wendt, A. N. Tiwari, Thin Solid Films **387**, 151 (2001).
[2] N. Amin, A. Yamada, M. Konagai, Japanese Journal of Applied Physics **41**(5A), Part 1 (2002).
[3] B. Ray, II-VI Compounds, Pergamon Press, Oxford (1969).

[4] C. Ferekides, J. Britt, Y. Ma, L. Killiam, Proceedings of the 23rd IEEE photovoltaic Specialists Conference, 1993, IEEE, Newyork, U.S.A.

[5] P. Capper, in: P. Capper (Ed.), Narrow-gap II-VI Compounds for Optoelectronic and Electromagnetic Applications, Chapman and Hall, New York (1997).

[6] F.A. Abouelfotouh, R.Al Awadi, M.M. Abd-Elnaby, Thin Solid Films **96**, 169 (1982).

[7] S.Chandrasekhar, S.Martinuzzi, F.Z.Nataren, Canadian Journal of Physics **63**, 716 (1985).

[8] P.R.Ram, R.Thangaraj, O.P. Agnihotri, Bulletin of Materials Science **8**, 279 (1986).

[9] K.T.R. Reddy, P.J. Reddy, Journal of Physics D: Applied Physics **25**, 1345 (1992).

[10] R.N. Bhattacharya, M.A. Contreras, B. Egaas, R.N. Noufi, A. Kanevce, J.R. Sites, Applied Physics Letters **89**, 253503/1 (2006).

[11] I.O. Oladeji, L. Chow, C.S. Ferekides, V. Viswanathan, Z. Zhao, SOLMAT. **61**, 203 (2000).

[12] K.L. Chopra, S.R. Das, Thin Film Solar Cell, Plenum Press, New York (1983).

[13] T.D. Dzhafarov, F. Ongul, I. Karabay, Journal of Physics D: Applied Physics **39**, 3221 (2006).

[14] Chu T L, Thin film cadmium telluride solar cells Final Technical Progress Report SERl sub-contract XL-3-03122-1, Dallas, Texas 1(1985).

[15] T. Yamaguchi, Y. Yamamoto, T. Tanaka, Y. Demizu, A. Yoshida, Thin Solid Films **375**, 281 (1996).

[16] T. Yamaguchi, J. Matsufusa, A. Yoshida, Japanese Journal of Applied Physics **3**, L703 (1992).

[17] J.J. Liou, Advanced Semiconductor Device Physics and Modelling, Artech House, Boston, (1994).

[18] I.O. Oladeji, L. Chow, C.S. Ferekides, V. Viswanathan, Z. Zhao, SOLMAT. **61**, 203 (2000).

[19] O.M. Hussain, P.S. Reddy, B.S. Naidu, S. Uthanna, P.J. Reddy, Sem. Sc. and Tech. **6**, 690 (1991).

[20] I.O. Oladeji, L. Chow, Thin Solid Films **474**, 77 (2005).

[21] M. Gunasekaran, M. Ichimura, Japanese Journal of Applied Physics **44**, 7345 (2005).

[22] J.H. Lee, W.C. Song, J.S. Yi, K.J. Yang, W.D. Han, J. Hwang, Thin Solid Films **431**, 349 (2003).

[23] O.P. Agnihotri, B.K. Gupta, Japanese Journal of Applied Physics **18**, 317 (1979).

[24] J. Zhou, X. Wu, G. Teeter, B. To, Y. Yan, R.G. Dhere, T. Gessert, Phy. St. Sol. **241**(3), 775 (2004).

[25] C. Ferekides, J. Britt, Y. Ma, L. Killian, Proceedings of the 23rd IEEE Photovoltaic Specialists Conference, 1993, IEEE, Louisville.

[26] A.L. Fahrenbruch, J .Aranovich, F. Courrages, S.Y. Yin, R.H. Buhe, Proc. Int. Photovoltaic Solar Energy Conf., 1977, Luxembourg, Dordrecht: Reidel.

[27] N. Suyama, N. Ueno, K. Omura, H. Takada, Y. Kita, S. Kitamura, T. Hibino, M. Murozono, Proc. 19th Photovoltaic Specialists Conf., 1987, IEEE, New Orleans, New York.

[28] S. J. Fonash, et al., www.cneu.psu.edu/amps, accessed in 2008.

[29] S. Degrave, M. Burgelman, and P. Nollet, Proceedings of 3rd World Conference on Photovoltaic Energy Conversion, May 11-18, 2003, Osaka, Japan.

[30] M. Gloeckler, A. L. Fahrenbruch, and J. R. Sites, Proceedings of the 3rd World Conf. on Photovoltaic Energy Conversion, May 11-18, 2003, Osaka, Japan.

[31] M. Burgelman, J. Verschraegen, S. Degrave, P. Nollet, Prog. Photovolt. Res. Appl., **12**, 143 (2004).

[32] M.A. Matin, Nowshad Amin and Kamaruzzaman Sopian, 2008 Regional Student Conference on Research and Development, November 26-27, SCOReD 2008, IEEE, UTM, Malaysia.

[33] N. Romeo, A. Bosio, R. Tedeschi, V. Canevari, Thin Solid Films **361-362**, 327 (2000).

[34] N. Romeo, A. Bosio, A. Romeo, Solar Energy Materials & Solar Cells (SOLMAT.) **94**, 2 (2010).

[35] M. A. Matin, Nowshad Amin, Azami Zaharim, Kamaruzzaman Sopian, Proceedings of the 8th WSEAS international conference on Non-linear analysis, 2009, La Laguna, Spain.

[36] M. A. Matin, Nowshad Amin, Aminul Islam, Kamaruzzaman Sopian, Kok-Keong Chong, 24th European Photovoltaic Solar Energy Conference, 21-25 September, 2009, Hamburg, Germany.

[37] M.A. Matin, Mannir Aliyu, Abrar H. Quadery, Nowshad Amin, Solar Energy Materials & Solar Cells **94**, 1496 (2010).
[38] M. Mahawela, G. Sivaraman, S. Jeedigunata, J. Gaduputi, M. Ramalingan, S. Subramanian, S. Vakklanka, C S. Ferekides, D.L. Morel, Material Science and Engineering **B 116**, 283 (2005).
[39] T.M. Razykov, Solar Energy Materials **12**, 233 (1985).
[40] T.M. Razykov, presented at the 7th International conference on Thin Films, 7-11 December, 1987, New Delhi, India (to be published in Thin Solid Films **164**, 301(1988).
[41] T.M. Razykov, B.KH. Kadyrov, M.A. Khodyaeva, Phys. Stat. Sol. **a 91**, K87 (1985).
[42] V.P. Singh, S. Singh, Czech. J. Phys. **b 26**, 1161 (1976).
[43] L.C. Burton, Solar Cells **1**, 159 (1980).
[44] X. Wu, Solar Energy **77**, 803 (2004).